Received March 1999
Revised February 2000
Accepted April 2000

Numerical simulation of the effect of thermal dispersion on forced convection in a circular duct partly filled with a Brinkman-Forchheimer porous medium

A.V. Kuznetsov and M. Xiong
Department of Mechanical and Aerospace Engineering, North Carolina State University, Raleigh, North Carolina, USA

Keywords *Numerical simulation, Porous media, Thermal dispersion*

Abstract *A numerical simulation of the fully developed forced convection in a circular duct partly filled with a fluid saturated porous medium is presented. The Brinkman-Forchheimer-extended Darcy equation is used to describe the fluid flow in the porous region. The energy equation for the porous region accounts for the effect of thermal dispersion. The dependence of the Nusselt number on a number of parameters, such as the Reynolds number, the Darcy number, the Forchheimer coefficient, as well as the thickness of the porous region is investigated. The numerical results obtained in this research are in agreement with published experimental data.*

Nomenclature

C = dimensionless experimental constant in representation of the effect of radial thermal dispersion
c_f = specific heat capacity of fluid, J/(kg·K)
c_F = Forchheimer coefficient
Da = Darcy number, K/r_o^2
d_p = average particle diameter in the porous region, m
F = scaled Forchheimer coefficient, $\frac{\rho_f C_F}{K^{1/2}} \frac{r_o^4}{\mu_f^2} G$
G = applied pressure gradient, $-d\tilde{p}/d\tilde{x}$, Pa/m
k_f = fluid thermal conductivity, W/mK
k_m = stagnant thermal conductivity of porous medium, W/mK
k_s = thermal conductivity of solid phase, W/mK
K = permeability, m^2
Nu = Nusselt number, $\frac{2r_o q''}{k_f(\tilde{T}_w - \tilde{T}_m)}$
$\tilde{p}$ = intrinsic average pressure, Pa
Pr = Prandtl number, $\frac{\nu \rho_f c_f}{k_f}$
q'' = wall heat flux, W/m^2
r = dimensionless radial coordinate, $\tilde{r}/r_o$
$\tilde{r}$ = radial coordinate, m
r_o = radius of the circular duct, m
r_{int} = radius of the clear fluid region, m
Re_d = particle Reynolds number based on mean velocity, $\frac{\tilde{U}_m d_p}{\nu_f}$
Re_p = particle Reynolds number based on characteristic velocity, $\frac{\left(\frac{Gr_o^2}{\mu f}\right) d_p}{\nu_f}$
R_{int} = dimensionless radius of the clear fluid region, r_{int}/r_o
T = dimensionless temperature, $\frac{\tilde{T} - \tilde{T}_w}{\tilde{T}_m - \tilde{T}_w}$
$\tilde{T}$ = fluid temperature, K
$\tilde{T}_m$ = mean flow temperature, $\frac{2}{r_o^2 \tilde{U}_m} \int_0^{r_o} \tilde{u}\tilde{T}\tilde{r}d\tilde{r}$, K
$\tilde{T}_w$ = wall temperature, K
u = dimensionless velocity, $\frac{\tilde{u}_f \mu_f}{Gr_o^2}$
$\tilde{u}_f$ = filtration (seepage) velocity, ms^{-1}

International Journal of Numerical Methods for Heat & Fluid Flow, Vol. 10 No. 5, 2000, pp. 488-501.

The authors acknowledge with gratitude the assistance of the North Carolina Supercomputing Center (NCSC) under an Advanced Computing Resources Grant.

U = dimensionless mean flow velocity, $\frac{\tilde{U}_m \mu_f}{Gr_o{}^2}$

$\tilde{U}_m$ = mean flow velocity, $\frac{2}{r_o{}^2}\int_0^{r_o} \tilde{u}\tilde{r}d\tilde{r}$, ms^{-1}

$\tilde{x}$ = streamwise coordinate, m

Greek letters

β = adjustable coefficient in the stress jump boundary condition

ε = porosity of the porous region

γ = constant characterizing viscosity ratio, $(\mu_{eff}/\mu_f)^{1/2}$

μ_f = fluid dynamic viscosity, $kgm^{-1}s^{-1}$

μ_{eff} = effective viscosity in the Brinkman term of the momentum equation for the porous region, $kgm^{-1}s^{-1}$

ρ_f = fluid density, kg/m^3

ν_f = fluid kinematic viscosity

1. Introduction

Considerable attention has recently been paid to the fluid flow and heat transfer in composite systems that are composed of regions filled either with a homogeneous fluid or with a fluid saturated porous medium. This interest is due to the wide use of these systems in engineering applications such as solar receiver devices, thermal insulation, heat exchangers, energy storage units, ceramic processing and catalytic reactors (Amiri and Vafai, 1994).

Studies in this field gradually progress towards complex models. At the beginning of these studies, a simple Darcy equation was used to describe the fluid flow in a porous medium. However, for high-speed flows it was found that that there is a deviation from the classical linear correlation between the pressure gradient and the filtration velocity, which is given by the Darcy equation. Then the so-called Darcy-Forchheimer equation, which includes a quadratic drag term to account for the deviation from linearity, was introduced. Further development of the model made by Brinkman was stimulated by a desire to impose the non-slip boundary condition at the solid wall (Nield and Bejan, 1999). It has recently become very popular to utilize the Brinkman-Forchheimer-Darcy equation, which accounts for both non-linear effects and viscous effects near the boundaries. Now this model is accepted and widely used (Vafai and Tien, 1981; Vafai and Thiyagaraja, 1987; Vafai and Kim, 1990; Amiri *et al.*, 1995; Amiri and Vafai, 1998; Hsieh and Lu, 1998; Nield and Bejan, 1999). Moreover, it has been found that thermal dispersion effects play an important role in forced convection in porous media (Amiri and Vafai, 1994; Plumb, 1983; Plumb and Whitaker, 1988a; 1988b; Hong and Tien, 1987; Hsu and Cheng, 1990). The models used to describe the transport phenomena in porous media are getting more and more sophisticated. The more complex the model is, the more difficult it is to get an accurate general theoretical solution. Poulikakos and Kazmierczak (1987) presented analytical solutions for fully developed forced convection in parallel plate channels and circular ducts partly filled with porous media. They utilized the Brinkman flow model and neglected thermal dispersion in the radial and transverse directions. Vafai and Kim (1989) obtained a boundary layer solution for a fully developed forced convection problem in a parallel plate channel filled with a Brinkman-Forchheimer porous medium. Nield *et al.* (1996) performed a theoretical analysis and obtained a solution for the same problem without utilizing the boundary layer approximation. Neither Vafai and Kim (1989) nor Nield *et al.* (1996) considered

the effect of thermal dispersion. In this paper the Brinkman-Forchheimer-Darcy equation is used as the momentum equation for the porous region and the radial thermal dispersion in the porous medium is accounted for in the energy equation for the porous region. Because of the geometrical configuration considered in this study and the presence of a non-linear term in the momentum equation, it is impossible to obtain an exact analytical solution for this problem. Thus, a numerical solution is adopted. The two cases of a constant heat flux and a constant wall temperature are investigated.

2. Problem formulation

The geometrical configuration considered in this research is displayed in Figure 1. Forced convection flow occurs in an infinite horizontal circular duct whose wall is subject to a uniform heat flux or a constant temperature. Assuming hydrodynamically and thermally fully developed flow, the governing equations for this problem are:

$$-\frac{d\tilde{p}}{d\tilde{x}} + \mu_f\left(\frac{d^2\tilde{u}_f}{d\tilde{r}^2} + \frac{1}{\tilde{r}}\frac{d\tilde{u}_f}{d\tilde{r}}\right) = 0 \qquad 0 \le \tilde{r} \le r_{int} \tag{1}$$

$$-\frac{d\tilde{p}}{d\tilde{x}} + \mu_{eff}\left(\frac{d^2\tilde{u}_f}{d\tilde{r}^2} + \frac{1}{\tilde{r}}\frac{d\tilde{u}_f}{d\tilde{r}}\right) - \frac{\mu_f}{K}\tilde{u}_f - \frac{\rho_f c_F}{K^{1/2}}\tilde{u}_f^2 = 0 \qquad r_{int} \le \tilde{r} \le r_o \tag{2}$$

$$\rho_f c_f \tilde{u}_f \frac{\partial \tilde{T}}{\partial \tilde{x}} = k_f\left(\frac{\partial^2 \tilde{T}}{\partial \tilde{r}^2} + \frac{1}{\tilde{r}}\frac{\partial \tilde{T}}{\partial \tilde{r}}\right) 0 \le \tilde{r} \le r_{int} \tag{3}$$

$$\rho_f c_f \tilde{u}_f \frac{\partial \tilde{T}}{\partial \tilde{x}} = \frac{1}{\tilde{r}}\frac{\partial}{\partial \tilde{r}}\left[\left(k_m + Ck_f\,Pr\frac{\rho_f \tilde{u}_f d_p}{\mu_f}\right)\tilde{r}\frac{\partial \tilde{T}}{\partial \tilde{r}}\right] r_{int} \le \tilde{r} \le r_o \tag{4}$$

where C is the dimensionless experimental constant, c_f is the specific heat capacity of the fluid, c_F is the Forchheimer coefficient, d_p is the average particle

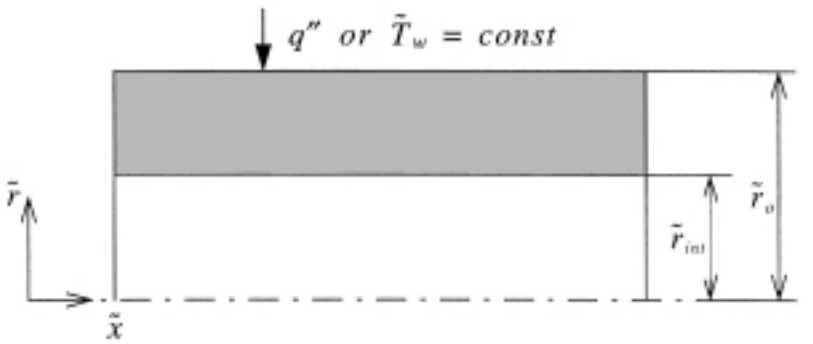

Figure 1.
Schematic diagram of the problem

diameter, K is the permeability of the porous medium, k_f is the thermal conductivity of the fluid, k_m is the stagnant thermal conductivity of the porous medium, r_o is the radius of the circular duct, r_{int} is the radius of the clear fluid region, $\tilde{T}$ is the temperature, $\tilde{u}_f$ is the filtration velocity, μ_{eff} is the effective viscosity of the porous medium, μ_f is the fluid viscosity, and ρ_f is the fluid density.

The Forchheimer coefficient, c_F, and the permeability, K, can be calculated utilizing formulas that are based on the results of experimental measurements carried out by Ergun (1952):

$$c_F = \frac{1.75}{\sqrt{150}\varepsilon^{3/2}} \tag{5}$$

$$K = \frac{\varepsilon^3 d_p^2}{150(1-\varepsilon)^2} \tag{6}$$

where ε is the porosity of the porous region.

The stagnant thermal conductivity of the porous medium, k_m, is calculated as:

$$k_m = \varepsilon k_f + (1-\varepsilon)k_s \tag{7}$$

where k_s is the thermal conductivity of solid phase.

Equations (1) and (2) are the momentum equations for the clear fluid and porous regions, respectively. In the porous region, the Brinkman-Forchheimer-extended Darcy equation is used. Equations (3) and (4) are the energy equations for the clear fluid and porous regions, respectively. The longitudinal heat conduction and longitudinal thermal dispersion are both neglected, which is justified if the Peclet number is large enough. Isotropy and homogeneity of the porous medium and local thermodynamic equilibrium in the porous region are assumed.

2.1 Constant heat flux

For the constant heat flux situation, equations (1)-(4) must be solved subject to the following boundary conditions:

$$\left.\frac{\partial \tilde{u}_f}{\partial \tilde{r}}\right|_{\tilde{r}=0} = 0 \qquad \left.\frac{\partial \tilde{T}}{\partial \tilde{r}}\right|_{\tilde{r}=0} = 0 \tag{8}$$

$$\left.\tilde{u}_f\right|_{\tilde{r}=r_{int}-0} = \left.\tilde{u}_f\right|_{\tilde{r}=r_{int}+0} \quad \mu_{eff}\left.\frac{\partial \tilde{u}_f}{\partial \tilde{r}}\right|_{\tilde{r}=r_{int}+0} - \mu_f\left.\frac{\partial \tilde{u}_f}{\partial \tilde{r}}\right|_{\tilde{r}=r_{int}-0} = \beta\frac{\mu_f}{K^{\frac{1}{2}}}\left.\tilde{u}_f\right|_{\tilde{r}=r_{int}} \tag{9a}$$

$$\left.\tilde{T}\right|_{\tilde{r}=r_{int}-0} = \left.\tilde{T}\right|_{\tilde{r}=r_{int}+0} \quad \left(k_m + Ck_f\,Pr\frac{\rho_f \tilde{u}_f d_p}{\mu_f}\right)\left.\frac{\partial \tilde{T}}{\partial \tilde{r}}\right|_{\tilde{r}=r_{int}+0} = k_f\left.\frac{\partial \tilde{T}}{\partial \tilde{r}}\right|_{\tilde{r}=r_{int}-0} \tag{9b}$$

$$\tilde{u}_f\big|_{\tilde{r}=r_o} = 0 \qquad \left(k_m + Ck_f\,Pr\frac{\rho_f \tilde{u}_f d_p}{\mu_f}\right)\frac{\partial \tilde{T}}{\partial \tilde{r}}\bigg|_{\tilde{r}=r_o} = q'' \tag{10}$$

where β is the dimensionless adjustable coefficient describing the jump in shear stress at the interface between the clear fluid and the porous medium (Ochoa-Tapia and Whitaker, 1995a; 1995b).

The governing equations (1)-(4) and boundary conditions (8)-(10) for the constant heat flux case can be recast into the dimensionless form by introducing the following dimensionless parameters:

$$u = \frac{\tilde{u}_f \mu_f}{Gr_o{}^2}, \quad U = \frac{\tilde{U}_m \mu_f}{Gr_o{}^2}, \quad T = \frac{\tilde{T} - \tilde{T}_w}{\tilde{T}_m - \tilde{T}_w}, \quad r = \frac{\tilde{r}}{r_o}, \tag{11a}$$

$$G = -\frac{d\tilde{p}}{d\tilde{x}}, \quad \gamma = \left(\frac{\mu_{eff}}{\mu_f}\right)^{1/2}, \quad F = \frac{\rho_f c_F}{K^{1/2}}\frac{r_o{}^4}{\mu_f^2}G, \quad Da = \frac{K}{r_o{}^2} \tag{11b}$$

where Da is the Darcy number, F is the scaled Forchheimer coefficient, and G is the applied pressure gradient.

In equation (11a), $\tilde{U}_m$ is the mean velocity and $\tilde{T}_m$ is the mean temperature of the flow. They are defined as:

$$\tilde{U}_m = \frac{2}{r_o{}^2}\int_0^{r_o} \tilde{u}\tilde{r}d\tilde{r} \tag{12}$$

$$\tilde{T}_m = \frac{2}{r_o{}^2\tilde{U}_m}\int_0^{r_o} \tilde{u}\tilde{T}\tilde{r}d\tilde{r} \tag{13}$$

For the constant heat flux (according to Bejan (1984)), the First Law of Thermodynamics results in the following relationship:

$$\frac{\partial \tilde{T}}{\partial \tilde{x}} = \frac{d\tilde{T}_m}{d\tilde{x}} = \frac{2}{r_o}\frac{q''}{\rho_f c_f \tilde{U}_m} \tag{14}$$

The dimensionless governing equations can now be presented as:

$$1 + \frac{d^2u}{dr^2} + \frac{1}{r}\frac{du}{dr} = 0 \qquad 0 \le r \le R_{int} \tag{15}$$

$$1 + \gamma^2\left(\frac{d^2u}{dr^2} + \frac{1}{r}\frac{du}{dr}\right) - \frac{1}{Da}u - Fu^2 = 0 \qquad R_{int} \le r \le 1 \tag{16}$$

$$-\frac{u}{U}Nu = \frac{d^2T}{dr^2} + \frac{1}{r}\frac{dT}{dr} \qquad 0 \le r \le R_{int} \tag{17}$$

$$-\frac{u}{U}Nu = \frac{1}{r}\frac{d}{dr}\left[\left(\frac{k_m}{k_f} + C \cdot Pr \cdot Re_p u\right) r \frac{dT}{dr}\right] \qquad R_{int} \le r \le 1 \tag{18}$$

where Nu is the Nusselt number defined by equation (19) below:

$$Nu = \frac{hD}{k} = \frac{2r_o q''}{k_f(\tilde{T}_w - \tilde{T}_m)} \tag{19}$$

Re_p in equation (18) is the Reynolds number based on the characteristic velocity scale, ${Gr_o}^2/\mu_f$, given by equation (20). An alternative would be to define the Reynolds number based on the mean flow velocity. In that case, however, the Reynolds number would depend on the solution, therefore using a characteristic velocity scale is preferable.

$$Re_p = \frac{\left(\frac{{Gr_o}^2}{\mu_f}\right) d_p}{\nu_f} \tag{20}$$

where ν_f is the kinematic viscosity of the fluid.

The dimensionless form of boundary conditions given by equations (8)-(10) is:

$$\left.\frac{du}{dr}\right|_{r=0} = 0 \qquad \left.\frac{dT}{dr}\right|_{r=0} = 0 \tag{21}$$

$$u|_{r=R_{int}-0} = u|_{r=R_{int}+0} \qquad \gamma^2 \left.\frac{du}{dr}\right|_{r=R_{int}+0} - \left.\frac{du}{dr}\right|_{r=R_{int}-0} = \frac{\beta}{\sqrt{Da}} u|_{r=R_{int}} \tag{22a}$$

$$T|_{r=R_{int}-0} = T|_{r=R_{int}+0} \qquad \left(\frac{k_m}{k_f} + C \cdot Pr \cdot Re_p u\right)\left.\frac{dT}{dr}\right|_{r=R_{int}+0} = \left.\frac{dT}{dr}\right|_{r=R_{int}-0} \tag{22b}$$

$$u|_{r=1} = 0 \qquad T|_{r=1} = 0 \tag{23}$$

In the energy equations (17) and (18), the Nusselt number is present as a parameter. Therefore, one more equation is needed to close this problem. This additional equation is given by the compatibility condition obtained from the definition of $\tilde{T}_m$ (Bejan, 1984):

$$\int_0^1 uTrdr = \frac{U}{2} \tag{24}$$

2.2 Constant wall temperature

The dimensional governing equations and boundary conditions for this case are similar to those for the isoflux case (equations (1)-(4) and (8)-(10)). The difference is that the second equation in equation (10) is replaced by:

$$\tilde{T}\big|_{\tilde{r}=r_o} = \tilde{T}_w \tag{25}$$

The dimensionless governing equations and boundary conditions for the flow velocity are the same as for the isoflux case and are given by equations (15), (16), (21), (22a) and (23). According to Bejan (1984), a pertinent relationship between $\frac{\partial T}{\partial \tilde{x}}$ and $\frac{\partial \tilde{T}_m}{\partial \tilde{x}}$ for the isothermal boundary condition is given by the following equation:

$$\frac{\partial \tilde{T}}{\partial \tilde{x}} = T\frac{d\tilde{T}_m}{d\tilde{x}} = T\frac{2}{r_o}\frac{q_w}{\rho_f c_f \tilde{U}_m} \tag{26}$$

This results in the following dimensionless energy equations for the clear fluid and porous regions, respectively:

$$-\frac{u}{U}NuT = \frac{d^2T}{dr^2} + \frac{1}{r}\frac{dT}{dr} \qquad 0 \le r \le R_{int} \tag{27}$$

$$-\frac{u}{U}NuT = \frac{1}{r}\frac{d}{dr}\left[\left(\frac{k_m}{k_f} + C \cdot Pr \cdot Re_p u\right) r\frac{dT}{dr}\right] \qquad R_{int} \le r \le 1 \tag{28}$$

The dimensionless boundary conditions for the temperature are also the same as those for the isoflux wall case, which are given by equations (21), (22b) and (23). Since the Nusselt number is present in the energy equations (27) and (28) as an unknown parameter, an additional equation is needed again to close the problem formulation. This additional equation follows from the definition of the Nusselt number:

$$Nu = -2\frac{k_m}{k_f}\frac{dT}{dr}\bigg|_{r=1} \tag{29}$$

3. Numerical procedure

Since there is a non-linear term in the momentum equation for the porous region, the equations are first written in the finite-difference form while the Newton iteration method is used to obtain the velocity field. Once the velocity distribution is found, it is easy to obtain the temperature distribution. For the

isoflux wall, T/Nu can be computed from equations (15)-(18) and (21)-(23). The Nusselt number can then be obtained by substituting the velocity distribution and T/Nu into equation (24).

In the case of the isothermal wall, it is important to avoid a trivial solution for the temperature. The same method as in Poulikakos and Kazmierczak (1987) and Nield *et al.* (1996) is utilized here. First, a value of the Nusselt number is guessed and equation (29) is utilized to obtain an expression for the first interior node near the wall. The temperature distribution for this Nusselt number is computed beginning from the wall and proceeding towards the duct center. Then the Newton iteration is used to adjust the Nusselt number and the process is repeated until the boundary condition at the center of the duct is satisfied.

4. Results and discussion

4.1 Constant heat flux

Figure 2 shows how the Nusselt number changes in relation to the Reynolds number, Re_d, according to these computations and shows a comparison of the numerical results with the experimental results obtained by Quinton and Storrow (1956). Since the experimental results given by Quinton and Storrow (1956) are reported in terms of Re_d, the numerical results obtained here are also given in terms of Re_d, where Re_d is the Reynolds number based on the mean flow velocity and is connected with previously utilized Re_p by the following correlation:

$$Re_d = U\, Re_p \tag{30}$$

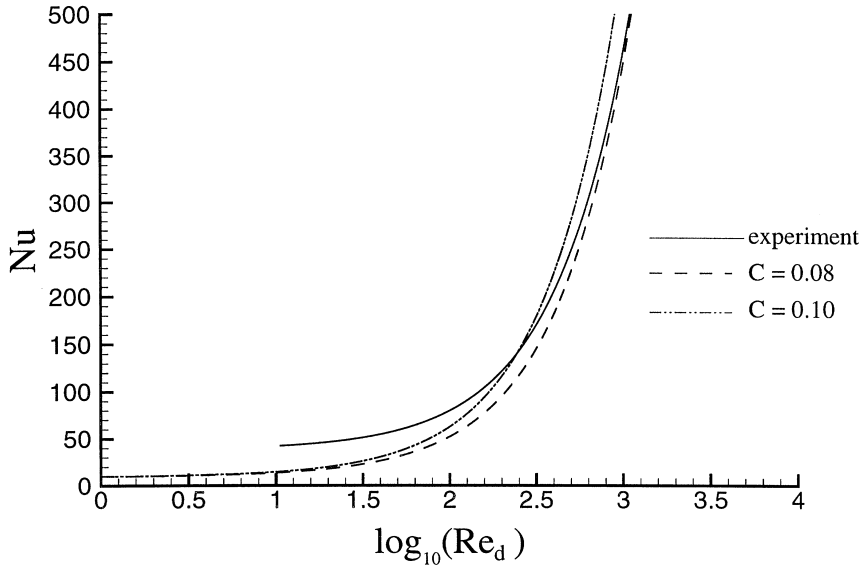

Figure 2.
Dependence of the Nusselt number on the particle Reynolds number for the case of an isoflux wall

The parameters utilized in the computation of Figure 2 are the same as in Quinton and Storrow (1956), $Da = 3.3895 \times 10^{-15}$, $F = 513.7467 \times Re_p$, $k_m/k_f = 1.2075$, $Pr = 0.7$, $R_{int} = 0.0$, $\varepsilon = 0.37$, and $\gamma = \frac{1}{\sqrt{\varepsilon}}$. For the constant C, two different values are utilized, $C = 0.08$ and $C = 0.1$ (0.1 is the value suggested in Wakao and Kaguei (1982)). When the Reynolds number is very small (of the order of unity), the Nusselt number does not depend on the Reynolds number and has an asymptotic value of 9.31. There is some difference between the numerical results and the experimental data for small Reynolds numbers. This is because longitudinal thermal dispersion is neglected in the computations, which can only be done for large Peclet numbers ($Pe = Pr \cdot Re$). If the Reynolds number is larger than 100, the Nusselt number increases rapidly with an increase in the Reynolds number and the numerical results agree well with the experimental data, especially in the case of $C = 0.08$.

Figure 3(a) displays the velocity distributions between the duct center and the wall for different values of the scaled Forchheimer coefficient, F, and the radius of the clear fluid region, R_{int}. As expected, an increase in the Forchheimer coefficient causes a decrease in the velocity distribution. This is because an increase in the Forchheimer coefficient means an increase in the resistance to the flow. It is also noticeable that when R_{int} is 0.25 there is a far-field region in the porous medium where the velocity does not change along the radius. This far-field region is located between the two momentum boundary layers, one of which is located near the solid wall and the other near the porous medium/clear fluid interface (Kuznetsov, 1996, 1998). When increasing R_{int} from 0.25 to 0.80, the velocity in the porous region stays nearly the same, but the velocity in the clear fluid region increases considerably. Since the presence of the porous medium heavily affects the fluid flow in the duct, it can be expected that it will also affect the heat transfer. Figure 3(b) displays the temperature distributions from the duct center to the wall. There is a kink at the interface, which in this case is caused by thermal dispersion in the porous medium. According to the second equation in (22b), thermal dispersion results in a discontinuity in the temperature gradient at the interface, even when stagnant thermal conductivity of the porous medium, k_m, is equal to the fluid thermal conductivity, k_f, as was assumed in computing of Figure 3(b).

The effect of the position of the clear fluid/porous medium interface on the Nusselt number is illustrated in Figure 4 for different values of the Darcy number and the Forchheimer coefficient. The case when $R_{int} = 0$ corresponds to the duct being completely filled with the porous medium. When most of the duct is filled with the porous medium ($R_{int} \leq 0.05$), the Nusselt number has nearly no dependence on R_{int}. When the duct is completely filled with clear fluid region, i.e. $R_{int} = 1$, the Nusselt number approaches 4.36, which coincides with the value given in Bejan (1984). Increasing the Darcy number causes an increase in the Nusselt number while increasing the Forchheimer coefficient causes a decrease in the Nusselt number. This is because a large Darcy number corresponds to a larger permeability of the porous medium, which translates to a larger filtration velocity, while a larger Forchheimer coefficient means a

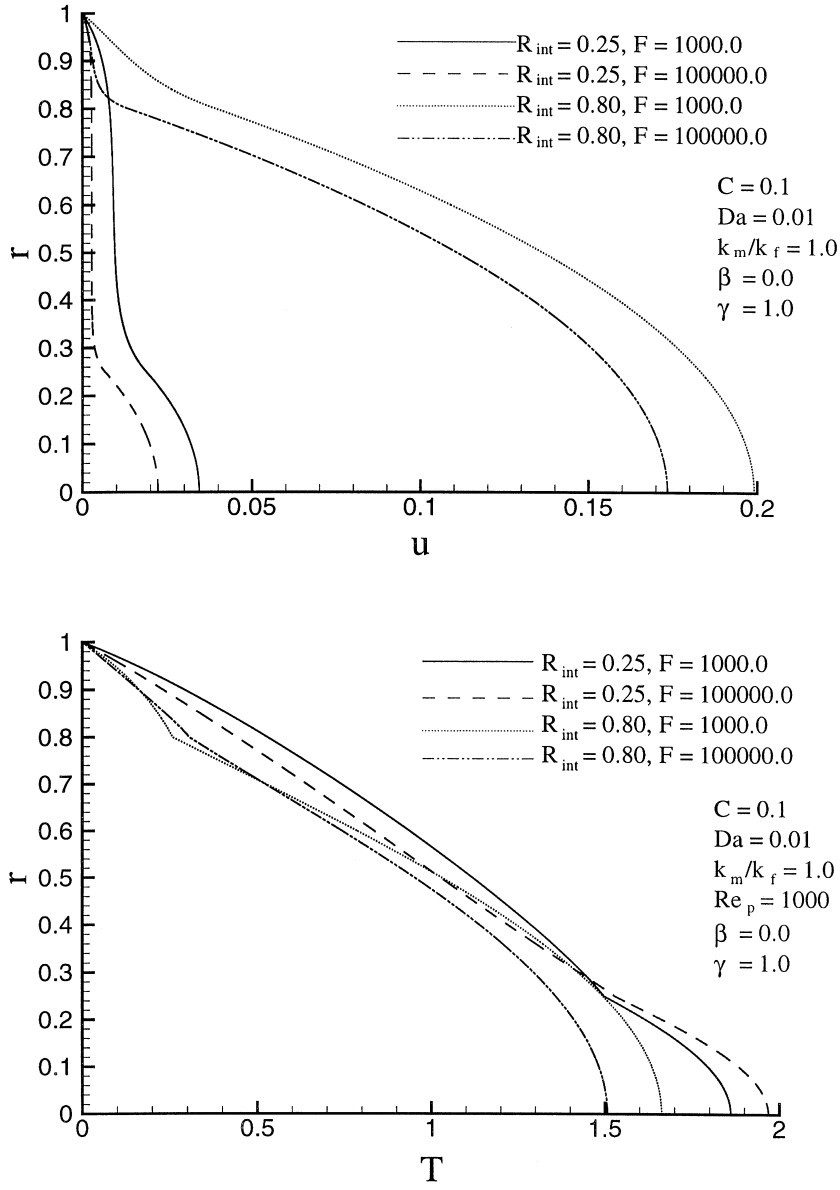

Figure 3.
Velocity and temperature distributions for different values of the Darcy number and Forchheimer coefficient for the case of an isoflux wall

stronger resistance to the flow, which translates to a small filtration velocity. When the Darcy number is of the order of 10^{-3} or less and the Forchheimer coefficient is of the order of 10^{3} or greater, the Nusselt number does not monotonically change with the thickness of the clear fluid region, but has a minimum value. This effect was first shown and explained in Poulikakos and Kazmierczak (1987).

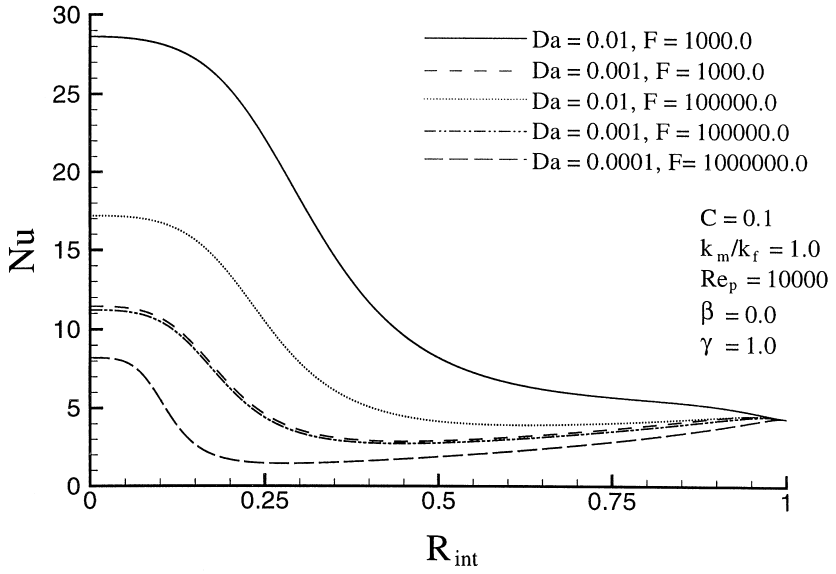

Figure 4.
Dependence of the Nusselt number on the thickness of the porous medium for the case of an isoflux wall

4.2 Constant wall temperature

Figure 5 depicts the change of the Nusselt number with the Reynolds number. To compare the numerical simulations with the experimental data of Verschoor and Schuit (1949), the parameter values used in this figure are the same as in Verschoor and Schuit (1949): Da = 1.867×10^{-4}, F = $106.27 \times Re_p$,

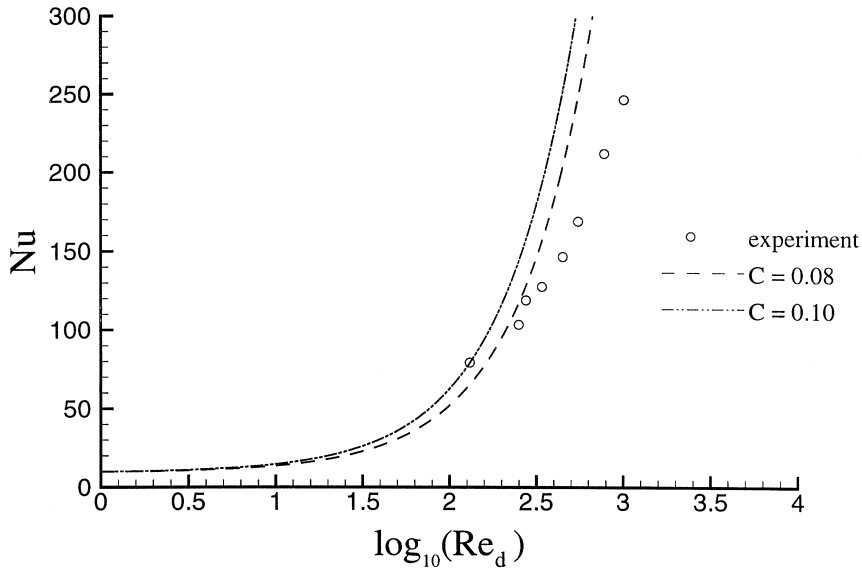

Figure 5.
Dependence of the Nusselt number on the particle Reynolds number for the case of an isothermal wall

$k_m/k_f = 5.481$, Pr = 0.7, $R_{int} = 0.0$, $\varepsilon = 0.412$, and $\gamma = \frac{1}{\sqrt{\varepsilon}}$. The results are similar to those for the isoflux case. The numerical results slightly overpredict the rate of increase of the Nusselt number when the Reynolds number is increased.

Figure 6 depicts the temperature distributions in the duct for different values of the Forchheimer coefficient for the isothermal wall. The parameters utilized to compute Figure 6 are the same as those used to compute Figure 3 for the isoflux wall case. The velocity distributions corresponding to the temperature distributions shown in Figure 6 are exactly the same as those for the isoflux wall case, which are shown in Figure 3(a). This is because the velocity distributions do not depend on the boundary condition for the temperature.

The dependence of the Nusselt number on the position of the clear fluid/porous medium interface is shown in Figure 7. The Nusselt number has the same trend as in the isoflux wall case (Figure 4), with the only difference being that the value of the Nusselt number in this case is slightly smaller than that in the isoflux case when computing for the same parameter values. When the whole duct is filled with a clear fluid, the numerically computed value of the Nusselt number is 3.65, which is very close to the value (3.66) given in Bejan (1984).

5. Conclusions

A numerical simulation of the forced convection in a circular duct partly filled with a Brinkman-Forchheimer porous medium is presented. The thermal dispersion effect is analyzed. Two kinds of thermal boundary conditions (isoflux wall and isothermal wall) are investigated. The trend of the Nusselt number variation with the parameters, such as the Darcy number, the scaled Forchheimer coefficient, the interface position, and the Reynolds number, is

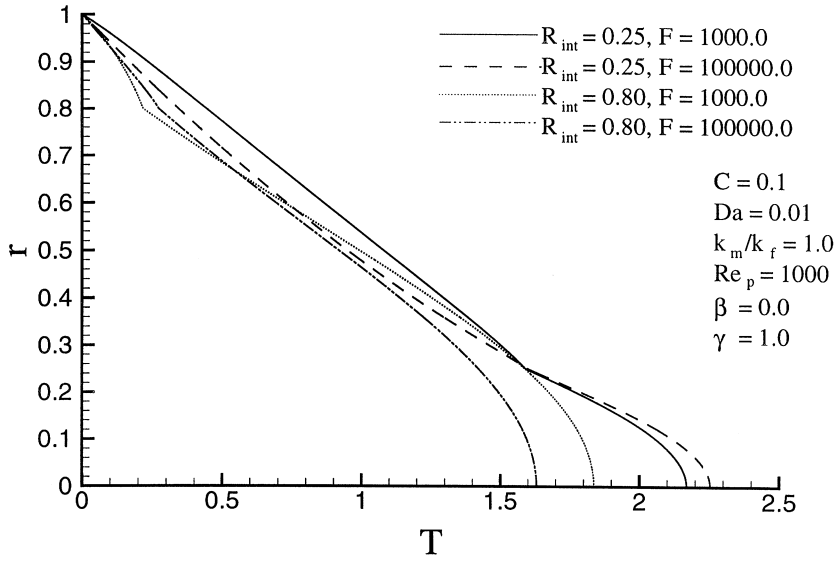

Figure 6.
Velocity and temperature distributions for different values of the Darcy number and Forchheimer coefficient for the case of an isothermal wall

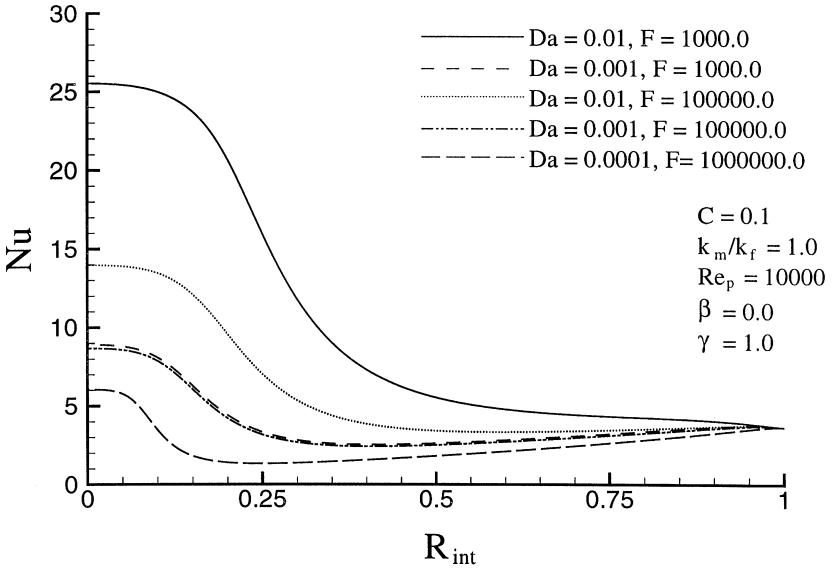

Figure 7.
Dependence of the Nusselt number on the thickness of the porous medium for the case of an isothermal wall

similar for both the isoflux and isothermal boundaries. The Nusselt number increases with an increase of the Reynolds number and does not change monotonically when the Darcy number is of the order of 10^{-3} or less and the Forchheimer coefficient is of the order of 10^{3} or greater. Increasing the Darcy number or decreasing the Forchheimer coefficient causes an increase in the Nusselt number. When the Darcy number is very small, the Forchheimer coefficient has only a weak effect on the Nusselt number.

References

Amiri, A. and Vafai, K. (1994), "Analysis of dispersion effects and non-thermal equilibrium, non-Darcian, variable porosity incompressible flow through porous media", *Int. J. Heat Mass Transfer*, Vol. 37, pp. 939-54.

Amiri, A. and Vafai, K. (1998), "Transient analysis of incompressible flow through a packed bed", *Int. J. Heat Mass Transfer*, Vol. 41, pp. 4259-79.

Amiri, A., Vafai, K. and Kuzay, T.M. (1995), "Effects of boundary conditions on non-Darcian heat transfer through porous media and experimental comparisons", *Numerical Heat Transfer*, Part A, Vol. 27, pp. 651-64.

Bejan, A. (1984), *Convection Heat Transfer*, Wiley, New York, NY.

Ergun, S. (1952), "Fluid flow through packed columns", *Chem. Engng. Prog.*, Vol. 48, pp. 89-94.

Hong, J.T. and Tien, C.L. (1987), "Analysis of thermal dispersion effect on vertical – plate natural convection in porous media", *Int. J. Heat Mass Transfer*, Vol. 30, pp. 143-50.

Hsieh, W.H. and Lu, S.F. (1998), "Heat-transfer analysis of thermally-developing region of annular porous media", *Heat Transfer*, Vol. 4, Proceedings of 11th IHTC, pp. 447-51.

Hsu, C.T. and Cheng, P. (1990), "Thermal dispersion in a porous medium", *Int. J. Heat Mass Transfer*, Vol. 33, pp. 1587-97.

Kuznetsov, A.V. (1996), "Analytical investigation of the fluid flow in the interface region between a porous medium and a clear fluid in channels partially filled with a porous medium", *Applied Scientific Research*, Vol. 56, pp. 53-67.

Kuznetsov, A.V. (1998), "Analytical study of fluid flow and heat transfer during forced convection in a composite channel partly filled with a Brinkman-Forchheimer porous medium", *Flow, Turbulence and Combustion*, Vol. 60, pp. 173-92.

Nield, D.A. and Bejan, A. (1999), *Convection in Porous Media*, 2nd ed., Springer-Verlag, New York, NY.

Nield, D.A., Junqueira, L.M. and Lage, J.L. (1996), "Forced convection in a fluid saturated porous-medium channel with isothermal or isoflux boundaries", *J. Fluid Mech.*, Vol. 322, pp. 201-14.

Ochoa-Tapia, J.A. and Whitaker, S. (1995a), "Momentum transfer at the boundary between a porous medium and a homogeneous fluid – I. Theoretical development", *Int. J. Heat Mass Transfer*, Vol. 38, pp. 2635-46.

Ochoa-Tapia, J.A. and Whitaker, S. (1995b), "Momentum transfer at the boundary between a porous medium and a homogeneous fluid – II. Comparison with experiment", *Int. J. Heat Mass Transfer*, Vol. 38, pp. 2647-55.

Plumb, O.A. (1983), "The effect of thermal dispersion on heat transfer in packed bed boundary layers", *Proc. ASME-JSME Thermal Engineering Joint Conference*, Vol. 2, pp. 17-22.

Plumb, O.A. and Whitaker, S. (1988a), "Dispersion in heterogeneous porous media – 1. Local volume averaging and large-scale averaging", *Water Resources Research*, Vol. 24, pp. 927-38.

Plumb, O.A. and Whitaker, S. (1988b), "Dispersion in heterogeneous porous media – 2. Predictions for stratified and two-dimensional spatially periodic system", *Water Resources Research*, Vol. 24, pp. 927-38.

Poulikakos, D. and Kazmierczak, M. (1987), "Forced convection in a duct partially filled with a porous material", *ASME Journal of Heat Transfer*, Vol. 109, pp. 653-62.

Quinton, J.H. and Storrow, J.A. (1956), "Heat transfer to air flowing through packed tubes", *Chemical Engineering Science*, Vol. 5, pp. 245-57.

Vafai, K. and Kim, S.J. (1989), "Forced convection in a channel filled with a porous medium: an exact solution", *ASME Journal of Heat Transfer*, Vol. 111, pp. 1103-6.

Vafai, K. and Kim, S.J. (1990), "Fluid mechanics of the interface region between a porous medium and a fluid layer – an exact solution", *Int. J. Heat Mass Transfer*, Vol. 30.

Vafai, K. and Thiyagaraja, R. (1987), "Analysis of flow and heat transfer at the interface region of a porous medium", *Int. J. Heat Mass Transfer*, Vol. 30.

Vafai, K. and Tien, C.L. (1981), "Boundary and inertia effect on flow and heat transfer in porous media", *Int. J. Heat Mass Transfer*, Vol. 24, pp. 195-203.

Verschoor, H. and Schuit, G.C.A. (1949), "Heat transfer to fluids flowing through a bed of granular solids", *Appl. Sci. Res.*, Vol. A2, pp. 97-119.

Wakao, N. and Kaguei, S. (1982), *Heat and Mass Transfer in Packed Beds*, Gordon and Breach, New York, NY.